Interactions of sucrose and trehalose with lysozyme in different media: a perspective from atomistic and coarse-grained molecular dynamics simulations

Inna Ermilova*,† and Jan Swenson†

Department of Physics, Chalmers University of Technology, SE 412 96, Gothenburg, Sweden

E-mail:

*Corresponding author: inna.ermilova@chalmers.se

Abstract

Disaccharides are promising additives for stabilizing proteins in, for example, pharmaceuticals and cryopreserved biomaterials. However, although many studies have shown that disaccharides exhibit such bioprotective and stabilizing properties, the underlying molecular mechanism is still elusive. In this study we have tried to reach such understanding by studying lysozyme in aqueous solutions of sucrose or trehalose and various ions (0.1 M of Cl^-, NaCl, $ZnCl_2$ and $CaCl_2$) by classical atomistic molecular dynamics (MD) and coarse-grained simulations. The latter simulations were performed for more diluted systems for elucidating larger structures of protein and disaccharide molecules, and possible aggregations. The most important finding for understanding the mechanism of protein stabilization is that the disaccharides in general, and

trehalose in particular, slow down the protein dynamics by reducing the number of internal hydrogen bonds (both with and without bridging water molecules) in the protein molecules. This reduction of internal protein interactions is caused by disaccharides binding to the protein hydration water, and trehalose forms more hydrogen bonds to water than sucrose. Although it is far from obvious that such a reduction of internal hydrogen bonding in the protein should lead to slower protein dynamics, and thereby also a stabilization of the protein, the results show that this is clearly the case. The presence of ions has also some effect on the protein dynamics and stability. Particularly, it is discovered that sucrose ability to prevent protein aggregation increases substantially if $ZnCl_2$ is added to the solution. The disaccharide and the salt seem to exhibit a synergistic effect in this case. To summarize, we have obtained molecular understanding for protein stabilization by disaccharides, and why trehalose is more effective than sucrose for this particular system, and the finding is important for understanding how the protein stability in e.g. pharmaceuticals should be optimized.

Introduction

Proteins are known to be important components in biological systems as well as ingredients of various pharmaceutical formulations.[1,2] Aggregation of these large molecules is undesired. In living organisms accumulated proteins can cause diseases while in formulations such clusters can result in a bad quality of products. An additional property which is not endorsed in industrial applications is the structural instability of these large molecules. Therefore, small molecules which can both inhibit the aggregation and stabilize structures are always of a high interest for diverse applications. Such molecules can be disaccharides, lipids etc.

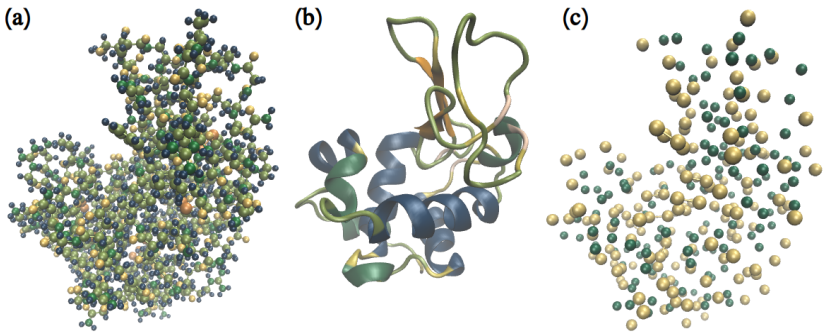

Figure 1: Lysozyme in various representations. (a) Atomistic. (b) Ribbons with secondary-structures. (c) Coarse-grained.

Disaccharides, in particular, sucrose and trehalose are already widely used in different formulations in pharmaceutical,[3] food[4] and cosmetic industries. For instance, sucrose is among components of famous mRNA-vaccines[5] against covid-19. Trehalose is the main component in eye drops Oxyal.[6] Nevertheless, despite the wide spreading utilization of disaccharides for every new formulation it is challenging to select the right one which would keep the product effective, safe and long lasting at its shelf.

When making a choice of a certain disaccharide various factors are taken into account. High cryoprotective effect is an important factor when using disaccharides in different formulations.[7] Storage and freeze-drying at very low temperatures of various pharmaceutical and cosmetic products can result in ice formation which can negatively affect the texture and other properties of those products.[8–10]

Another such a factor is an ability of a disaccharide to preserve the structure.[11] It can be a structure of a large biomolecule, but it can also be an object containing many different types of molecules, like lipid nano-particle (LNP) or a biomembrane.[12–14]

The third desirable function of a disaccharide is its ability to prevent aggregation of molecules or groups of molecules (for example, LNPs in some solution). Keeping molecules or LNPs separated from each other can be a key to the efficacy of a certain formulation.[15–17]

In this work sucrose and trehalose together with an egg protein lysozyme are considered in a computational study by all-atom and coarse-grained molecular dynamics simulations.

Lysozyme is selected as a popular model-protein which was well-studied by various experimental techniques. It is a globular protein[18] that can be found in for example tears, saliva and milk.[19] In humans, lysozyme is a vital part of the immune system as it damages and kills bacteria through multiple mechanisms, such as hydrolyzing specific residues in the peptidoglycan of bacterial cell walls.[20] The hen egg lysozyme is similar to the human lysozyme, but while the human variant consists of 130 amino acids, the hen egg type has 129 amino acids.[21] The polypeptide chain is structurally stabilized by four disulfide bonds,[22,23] and include two domains; one dominated by *β-sheets* and another composed of mostly *α-helices*.[23–25] Located between the two domains is the active site.[25,26] The structure of the hen egg lysozyme 7VGO[27] is visualized in Figure 1.

This protein was always very attractive for experimental studies for various reasons. Considering its properties, perhaps, the reversibility of its denaturation[28] in a liquid state is of most interest for biophysicists and biochemists. Lysozyme's therapeutic properties are also intriguing due its anticancer[29] and antiviral[30] activities. For laboratory scientists this protein is one of the cheapest and most available models.[31–33] Therefore, there have been an extensive research in experimental biophysical chemistry regarding lysozyme.[28,34–39]

Results from experimental works have various suggestions on which disaccharide to select for formulations, but no precise mechanisms of interactions were disclosed.[39] Knowledge of those mechanisms would help to optimize future formulations.

Then advanced molecular simulations are right tools for providing such a help in comprehension of behaviors of pharmaceutical proteins in mixtures with disaccharides. Results from modeling can also be utilized for the explanation of potential choice of either sucrose or trehalose for a selected ratio of compounds.

Lysozyme in mixtures with disaccharides (with sucrose, trehalose and maltose) was studied earlier by A. Lerbret et al.,[40] but each mixture contained only one protein molecule which gives no information about possible interactions between proteins. In their results it was revealed that trehalose was more excluded from the protein surface than maltose and

sucrose.

Trehalose-protein interactions where lysozyme was used as a model were the topic of work by R. D. Lins et al.[41] 0.5 M concentration of the disaccharide was utilized in the presence of a single protein. They concluded that trehalose was not completely dehydrating lysozyme, but it was acting as a coating for it.

M. V. Fedorov et al.[42] investigated aqueous mixtures of lysozyme and trehalose. Their simulations were also designed for single proteins. It was discovered that trehalose binds to the surface of lysozyme, but, again, there was no information about inter-protein interactions.

M. Simončič et al.[43] also simulated single lysozyme molecules, but with sucralose and sucrose. They found that sucralose was a better preservative for the protein than sucrose.

In contrary to previous works, in this project larger systems are considered for modeling. Atomistic MD simulations are performed for 4 proteins in each mixture. This can help to understand if disaccharides can inhibit the aggregation of lysozyme. Counter ions of Cl^- and salts (NaCl, $ZnCl_2$) are used for finding out how they can affect the protein dynamics and the different interactions between the protein, disaccharide and water.

Furthermore, a set of coarse-grained simulations is being utilized for investigating potential formations of larger structures. In particular, here 16 proteins are being used in more diluted solutions than in atomistic simulations, because a single water-bead stands for 4 water molecules. Due to limits of computational resources, running coarse-grained modeling can help to reach time- and size-scales which can not be accessible with atomistic MD. The time of 66 μs was set for these low resolution simulations.

Methods and models

All-atom MD simulations

Starting configurations were designed in the following way. In cubic boxes with the side of 25 nm 4 proteins were randomly placed keeping the distance of around 1 nm between them in

order to avoid initial aggregation due to too close locations. Then disaccharides were added in boxes containing only 4 proteins. Model for the protein was taken from the CHARMM36[44] force field, while models for disaccharides were taken from work by K. Ahlgren et al.[45]

After the addition of disaccharides water of TIP3p[46,47] and ions were added, where the amount of ions was equal to the concentration of 0.1M NaCl (which is not valid for counter ions of Cl^-, used for neutralizing the total charge of the system). The idea was to design systems corresponding to the following mass ratios:

- m(Lysozyme):m(Water)=1:2.7;

- m(Lysozyme):m(Sucrose/Trehalose):m(Water)=1:1.3:2.7.

Final compositions of the systems are presented in Table 1.

Table 1: Compositions of simulated systems using atomistic models. For simplifying the discussion systems will be labeled with abbreviations: LYS. - lysozyme, SUC. - sucrose, TRE. - trehalose.

System	Number of disaccharides	Number of positive ions	Number of negative ions	Number of water molecules
LYS.	0	0	32	8596
LYS.+SUC.	223	0	32	8478
LYS.+TRE.	223	0	32	8478
LYS.+NaCl	0	35	67	8596
LYS.+SUC.+NaCl	223	34	66	8478
LYS.+TRE.+NaCl	223	34	66	8478
LYS.+$ZnCl_2$	0	18	68	8596
LYS.+SUC.+$ZnCl_2$	223	17	66	8478
LYS.+TRE.+$ZnCl_2$	223	17	66	8478

Before running actual production runs every system was equilibrated, using GROMACS-2019[48] as an MD engine. Production runs were performed in the NPT[49] ensemble using the isotropic pressure coupling scheme for 200 ns with a time-step of 2 fs and the integrator leap-frog.[50] Berendsen[51] barostat was utilized to maintain a pressure of 1.013 bar with a coupling constant of 10 ps and a compressibility of $4.5 \cdot 10^{-5}$ bar^{-1}. The temperature was kept at 310.15 K by Velocity Rescale[52] thermostat with a coupling constant of 0.5 ps. A cut-off distance of 1.2 nm was employed for Coulumb, Lennard-Jones and short-range

neighbor interactions with the cutoff scheme Verlet.[53] The trajectory was recorded every 4 ps. LINCS[54] algorithm with 12 iterations was utilized for constraining bonds. Long-range electrostatics was handled by the Particle Mesh Ewald[55] algorithm.

Last frames from equilibrations were used as starting configurations for production runs with the NVT[56] ensemble. Every simulation was 500 ns long and the output for the trajectory was made every 2 ps. All other settings including thermostat and relevant constant were the same as during the equilibration, except that barostat was not used.

Coarse-grained MD simulations

Firstly, protein structures were processed by CHARMM-GUI[57] in order to get coarse-grained architecture suitable for the MARTINI[58] force field.

Then resulting pdb-structures were placed in cubic boxes with a side of 40 nm, where the number of lysozyme molecules was equal to 16. When placing proteins in a box a distance of around 1 nm between them was used in order to avoid aggregation in the beginning of the simulation. Then other molecules (disaccharides and water) and ions of salts were randomly placed in the boxes.

In coarse-grained simulations Ca^{2+} was used instead of Zn^{2+} as there was no available model for Zn^{2+} ions in the MARTINI[58] force field. All systems were designed with either NaCl or $CaCl_2$. There were no simulations with only counter ions of Cl^- like in the atomistic modeling.

Final system compositions can be seen in Table 2.

Table 2: Compositions of simulated systems using coarse-grained models. For simplifying the discussion systems will be labeled with abbreviations: Lys. - lysozyme, Suc. - sucrose, Tre. - trehalose.

System	Number of disaccharides	Number of positive ions	Number of negative ions	Number of water molecules
Lys.+NaCl	0	140	268	34384
Lys.+Suc.+NaCl	892	136	264	34384
Lys.+Tre.+NaCl	892	136	264	34384
Lys.+$CaCl_2$	0	72	272	34384
Lys.+Suc.+$CaCl_2$	892	68	264	34384
Lys.+Tre.+$CaCl_2$	892	68	264	34384

As in the atomistic simulations, the software was GROMACS-2019[48] . All systems were going through energy minimizations using the steepest descent algorithm in order to prevent overlaps of particles. Then every system was simulated using NPT[49] ensemble with Berendsen[51] barostat and isotropic pressure coupling with a constant of 5 ps, compressibility of $3 \cdot 10^{-4}$ bar^{-1} and a pressure of 1 atm. The temperature was held by Velocity rescale[52] thermostat with a coupling constant of 1 ps and a reference temperature of 310.15 K. The integrator for solving Newtonian equation of motions was leap-frog[50] with a time-step of 20 fs. The electrostatics was handled by the Reaction-Field[59–61] algorithm with a dielectric constant (epsilon-r) of 15. The distance for coulombic cutoff was 1.1 nm. The cutoff scheme was Verlet[53] with Verlet buffer tolerance equal to 0.005 kJ/(mol$\cdot$ ps). Long-range van der Walls interactions are taken care of by the cutoff type and by a modifier Potential-Shift-Verlet[48] with a distance of 1.1 nm. Peridodic boundary conditions were used in x, y and z directions. This equilibration was for 160 ns. Then the last frame was taken for further equilibration and a production run.

All settings for production runs were the same as in the previous "step", except that here the run was 66 μs. The pressure coupling algorithm was Parinello-Rahman[62–64] with a coupling constant of 12 ps.

Statistical software and calculations

For performing analysis of simulated data statistical tools from programming language Python-3 were used. In particular routines from packages *NumPy*, *SciPy* and *matplotlib* were utilized for statistical calculations and plotting of graphs.[65,66]

For calculations of correlations Pearson's and Spearman's correlation coefficients were used.

Pearson's correlation[67,68] coefficient is used to measure the linear correlation between two datasets. Where absolute values between 0.5 and 1 suggest strong correlation, values in the range 0.3 and 0.49 indicate moderate correlation, weak correlation can be concluded from coefficients in the range below 0.29 and no correlation can be deduced from values close to 0.

Spearman's correlation[67,69] coefficient is applied for finding out the monotonicity of the relationship between two datasets. The classification is similar to the one used for Pearson's correlation coefficient.

For each correlation coefficient its P-value is utilized, which is the value of the probability that the computed correlation is coming from an uncorrelated dataset, meaning that the coefficient is false.

Results

All-atom MD simulations

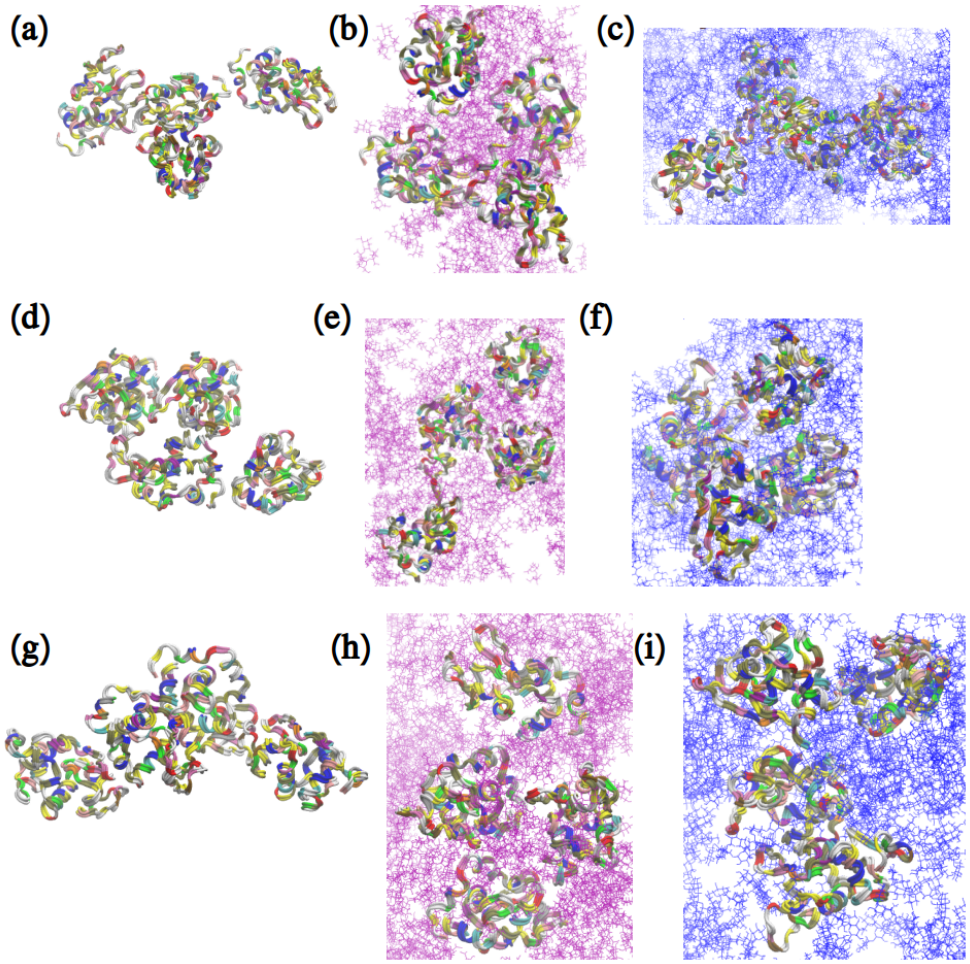

Figure 2: Snapshots from atomistic MD simulations of the following systems. (a) LYS. (b) LYS.+SUC. (c) LYS.+TRE. (d) LYS.+NaCl. (e) LYS.+SUC.+NaCl. (f) LYS.+TRE.+NaCl. (g) LYS.+$ZnCl_2$. (h) LYS.+SUC.+$ZnCl_2$. (i) LYS.+TRE.+$ZnCl_2$. Water and ions are omitted for clarity. Proteins are presented as ribbons. Sucrose and trehalose are presented as thin purple and blue molecules respectively.

Before discussing statistical results it is important to give a look at snapshots from the last frames of the systems. Figure 2 demonstrates snapshots for all systems. Regardless of what ions were present in each system, lysozyme appears to be aggregated in each aqueous solution (Figure 2 (a), (d), (g)). The disaccharides separate the protein molecules but there are no significant visual differences in snapshots between the systems containing sucrose or

trehalose.

Root mean-square deviation (RMSD) and radius of gyration

RMSD tells us about how similar two protein structures are by comparing their superimposed atomic coordinates. High values of RMSD indicate large changes in structure compared to the reference structure. The statistics over time also provides information about the dynamics of lysozyme.

In order to find out how stable proteins are in each mixture, RMSDs for every single chain of lysozyme were computed and presented in Figures S1-S3 of the Electronic Supporting Information (ESI). The average RMSD profiles for all proteins in each system are shown in Figure 3. Lysozyme in aqueous solutions without disaccharides appears to be most unstable due to the highest values of RMSD. For systems with only counter chloride ions there is basically no difference in the RMSD of lysozyme between the two disaccharide containing systems. Presence of NaCl makes trehalose a better preservative, due to smaller values of RMSD, compared to sucrose. In solutions with $ZnCl_2$ the presence of disaccharides does not seem to play a big role, because RMSDs for all 3 systems appears to be similar. Nevertheless, all observed fluctuations of RMSD were not dramatic as values were oscillating in the range of 0.1-0.2 nm.

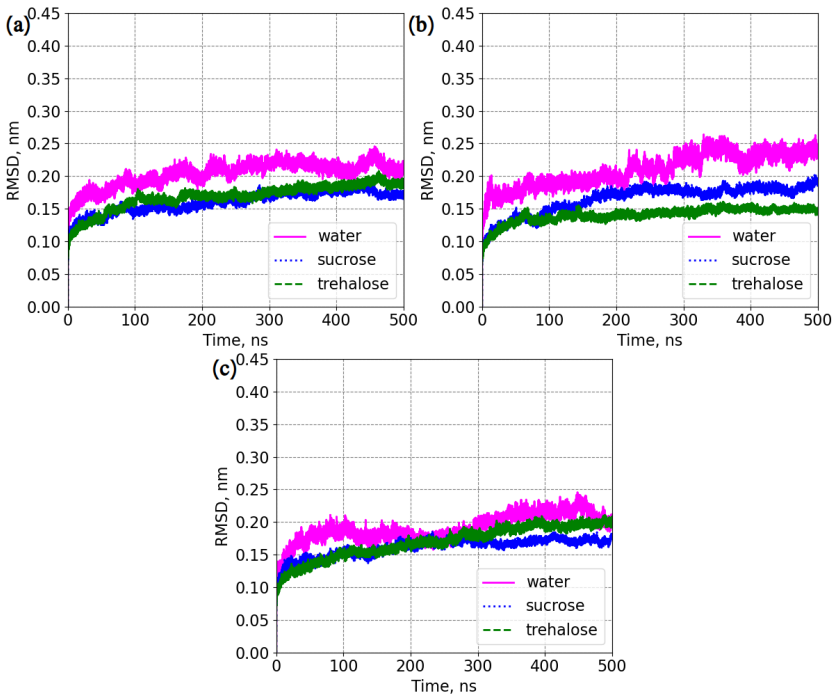

Figure 3: Average RMSD for lysozyme. (a) Systems: LYS., LYS.+SUC., LYS.+TRE. (b) Systems: LYS.+NaCl, LYS.+SUC.+NaCl, LYS.+TRE.+NaCl. (c) Systems: LYS.+$ZnCl_2$, LYS.+SUC.+$ZnCl_2$, LYS.+TRE.+$ZnCl_2$. "Water" stands for systems without disaccharides. RMSD was computed for each protein molecule and then averaged over the 4 molecules.

The evolution of the radius of gyration was also computed for the protein (Figures S4-S7 in ESI). In all simulated systems differences in values were rather negligible.

Self-intermediate scattering functions and relaxation times

Self-intermediate scattering functions (SISF) give additional information about the mobility of the molecules in the system. They are calculated from the self-part of the van Hove's function.[70–72] For a protein the most essential part, responsible for its secondary structure is the backbone. Therefore, to determine whether disaccharides can stabilize protein molecules it is enough to calculate backbone relaxation times from SISFs for some selected values of the scattering vector q.

Figure 4 demonstrates relaxation times for 4 selected q-values for the backbone of the protein. The values were obtained by fitting a single exponential function to each SISF (as

it was done by J. Gilbert et al.[73]), presented in Figures S8-S11. Lysozyme has the fastest dynamics in aqueous solutions without disaccharides, while in the presence of trehalose it has the slowest dynamics.

The presence of ions also affect the motion of lysozyme. In solutions without disaccharides the protein's backbone has the slowest dynamics in the presence of $ZnCl_2$ and it relaxes faster with NaCl. With disaccharides the protein's backbone has the slowest dynamics when only Cl counter ions are added and it has the shortest relaxation times with NaCl.

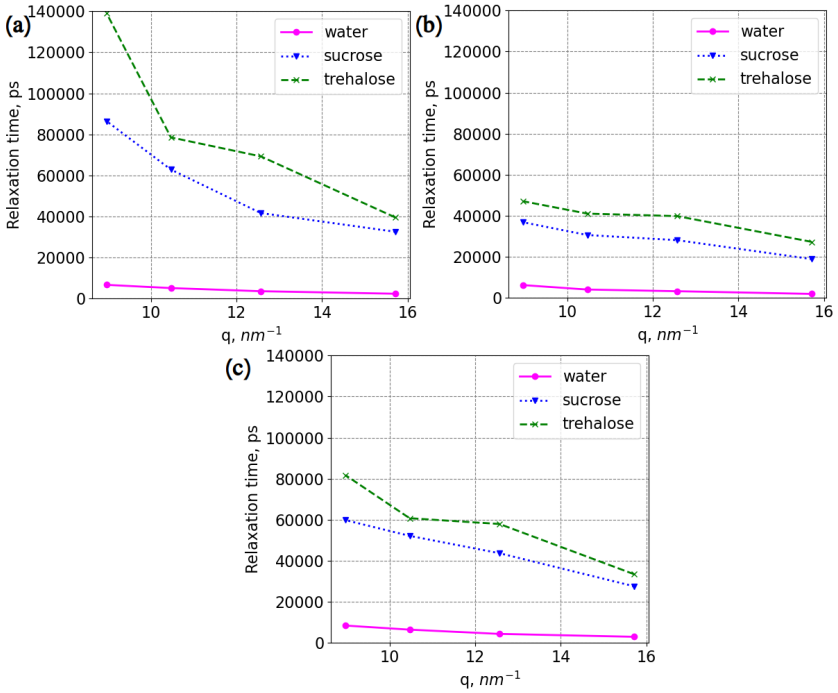

Figure 4: Relaxation times for the backbone of lysozyme. (a) Systems: LYS., LYS.+SUC., LYS.+TRE. (b) Systems: LYS.+NaCl, LYS.+SUC.+NaCl, LYS.+TRE.+NaCl. (c) Systems: LYS.+$ZnCl_2$, LYS.+SUC.+$ZnCl_2$, LYS.+TRE.+$ZnCl_2$. "Water" stands for systems without disaccharides. Error bars are within markers.

Hydrogen bonds, total number of contacts and radial distribution functions (RDFs)

Hydrogen bonding plays a key-role for the behavior of the simulated systems. The protein structure depends on hydrogen bonds between amino-acid residues. Figure 5 shows hydrogen bonds between different molecules in the modelled mixtures.

When considering protein-protein hydrogen bonds it is important to distinguish between inter- and intra-molecular ones. The number of inter-molecular hydrogen bonds (Figure 5(a)) tells us about the affinity between different lysozyme molecules (each simulation had 4 of them). In systems without disaccharides these numbers are the highest, because there is no hinder for potential binding. In the presence of sucrose and $ZnCl_2$ the protein molecules are almost perfectly separated, as the number of hydrogen bonds is close to 0, while trehalose is less successful in the presence of the same salt. Instead, trehalose inhibits protein aggregation best in the mixture with NaCl, where sucrose is not able to separate different lysozyme molecules. In the presence of only counter ions of Cl both disaccharides perform similarly. Regarding the higher ability of sucrose in the presence of $ZnCl_2$ to separate protein molecules, it is important to note that there are less hydrogen bonds on average in an aqueous solution of lysozyme and $ZnCl_2$, compared to a pure aqueous solution of lysozyme. This implies that the efficacy of sucrose is a result of synergistic effects of the disaccharide and the salt. In fact, in a recent experimental work A. Rogowska et al.[74] discovered that Zn^{2+} ions could stabilise hen egg white lysozyme.

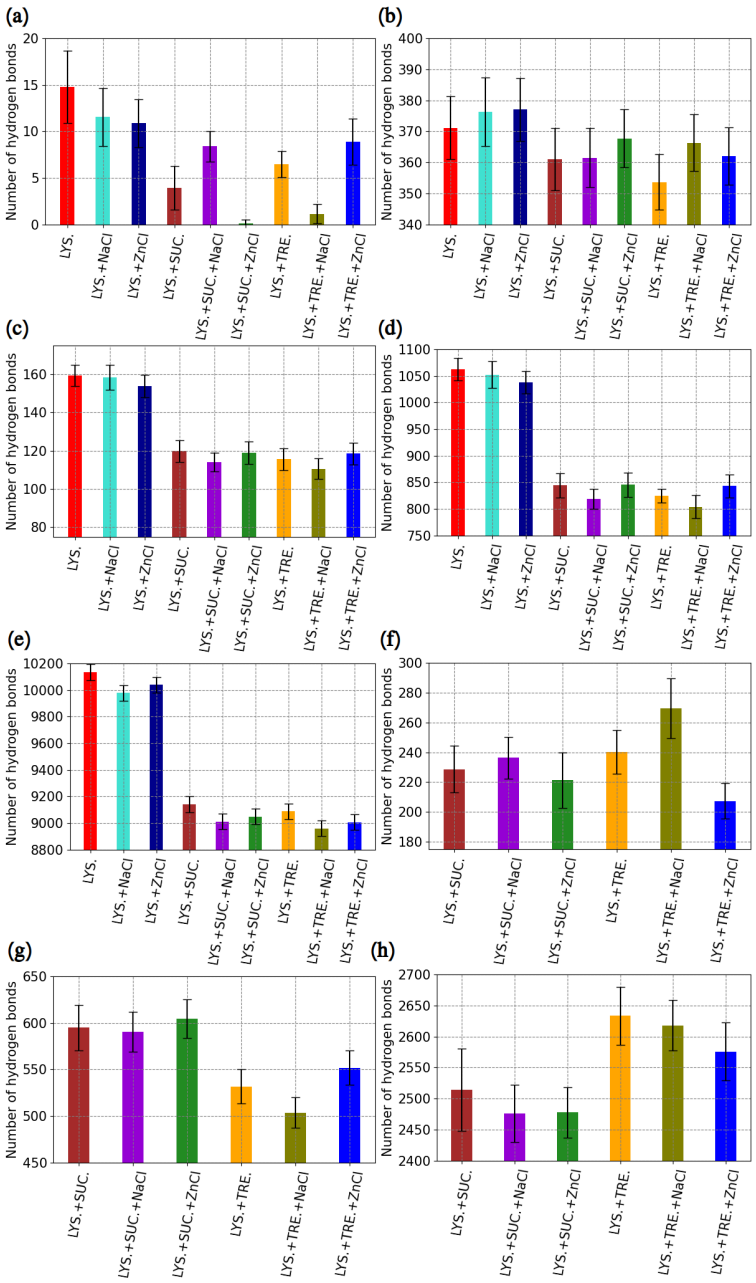

Figure 5: Average number of hydrogen bonds in the systems. (a) Protein-protein: intermolecular. (b) Protein-protein: intra-molecular. (c) Protein-water-protein (here values are per 1 protein molecule): bridging intra-protein bonds with water. (d) Protein-water. (e) Water-water. (f) Protein-disaccharide. (g) Disaccharide-disaccharide. (h) Disaccharide-water. Systems' names are on x-axis named after Table 1. Error-bars represent the standard deviation. The standard error was 0.02% for every simulation. In figure's legend on x-axis "ZnCl" is used as an abbreviation for $ZnCl_2$. Average numbers of protein-water and water-water hydrogen bonds per water molecule, corresponding to (c), (d) and (e), are presented in Figure S12 of ESI.

Intra-molecular hydrogen bonds have another importance for preserving the protein structure as their internal network is responsible for holding secondary structures. There are more internal hydrogen bonds within lysozyme in mixtures without disaccharides (Figure 5(b)). However, within the large standard deviations there is no significant difference in the number of hydrogen bonds between the sucrose and trehalose containing systems, despite that the average values for trehalose are smaller than for sucrose in all systems except those with NaCl.

The internal structure of proteins in the presence of water is also held by hydrogen bridging bonds or so-called bifurcated[75–77] hydrogen bonds. They are formed between parts of lysozyme where water with ions are playing roles of connecting atoms. The only way to isolate such hydrogen bonds is by creating new index-files with the following groups: for each protein molecule a separate group is made (4 groups), then a group with each protein molecule including water and ions is created (4 groups). The resulting values of protein-water-protein (this name is chosen for intra-molecular bonds of a protein, which occur through atoms of water molecules, acting as connecting units for the internal structure of lysozyme) bridging hydrogen bonds are computed using the following equation (1):

$$HB_{intra,p-w-p,bridging} = \frac{1}{4}(\sum_{i=1}^{4} HB_{intra,p+w,i} + \sum_{i=1}^{4} HB_{intra,p,i}) - HB_{w-w} \quad (1)$$

Here "intra" stands for intra-protein, "p" - protein, "w" - water and ions, "HB" number of hydrogen bonds. Since the resulting value is divided by the number of lysozyme molecules (which equals to 4) before the number of water-water hydrogen bonds is subtracted, it gives us the average number of bridging hydrogen bonds per protein molecule. Computed values are shown in Figure 5(c). From the figure it follows that in systems without disaccharides there are more bridging hydrogen bonds in the internal structure of the protein. From the average values it can be concluded that in mixtures of trehalose the number of such hydrogen bonds is slightly smaller than in the presence of sucrose, although the differences are within the standard deviations. The addition of $ZnCl_2$ results in a decrease of the number of

bridging hydrogen bonds in the system without disaccharides, and the highest number of such bonds is obtained for the sample with only counter ions of Cl^-. However, also in this case the differences are sufficiently small to be within the standard deviations.

Similar calculations were done replacing water and ions with disaccharides in order to investigate whether they are forming bridging bonds within the protein. However, that was not the case probably due to their larger size compared to water molecules.

Considering further interactions of lysozyme with water and ions, from Figure 5(d) is can be concluded that disaccharides significantly decrease the number of protein-water hydrogen bonds, compared to the corresponding systems without them. This can be explained by binding of sucrose and trehalose to lysozyme molecules (Figure 5(f)), where from the average numbers of hydrogen bonds can be concluded that $ZnCl_2$ inhibits associations between disaccharides and protein, while NaCl promotes it.

As water and ions affect the behavior of proteins and disaccharides, the latter ones can also influence the interactions within water and ions. Figure 5(e) presents hydrogen bonds between water molecules in each system. The highest number of hydrogen bonds is obtained for mixtures without disaccharides, where the highest average value is for the system with only counter ions of Cl^-. In mixtures without disaccharides the lowest average number of water-water hydrogen bonds is observed for the system with NaCl. Comparison of systems with either sucrose or trehalose, shows that in the presence of trehalose the average number of hydrogen bonds between water molecules was smaller than in mixtures with sucrose. The smallest average value of water-water hydrogen bonds is found for lysozyme with trehalose and NaCl while the highest one is observed for lysozyme with sucrose and counter ions of Cl^-.

From differences between numbers of protein-water (Figure 5(d)) and protein-disaccharide (Figure 5(f)) hydrogen bonds it can be concluded that there still is a preferential hydration of the protein. Moreover, trehalose and sucrose have a tendency to bind water themselves, where sucrose binds less water than trehalose (Figure 5(h)).

The disaccharides also form some hydrogen bonds with each other (Figure 5(g)), where there are more sucrose-sucrose hydrogen bonds than trehalose-trehalose. This is coherent with earlier findings by I. Ermilova et al.[78]

The number of contacts between amino-acid residues is another characteristic which can explain possible mechanisms of interactions in the studied systems. Figure 6 and Table 3 demonstrate average numbers of contacts per amino-acid residue. The figure shows that there are more contact points within the protein molecules in mixtures without disaccharides, although Table 3 shows that there are no dramatic differences in numbers of contacts among the systems if the standard deviations are taken into account.

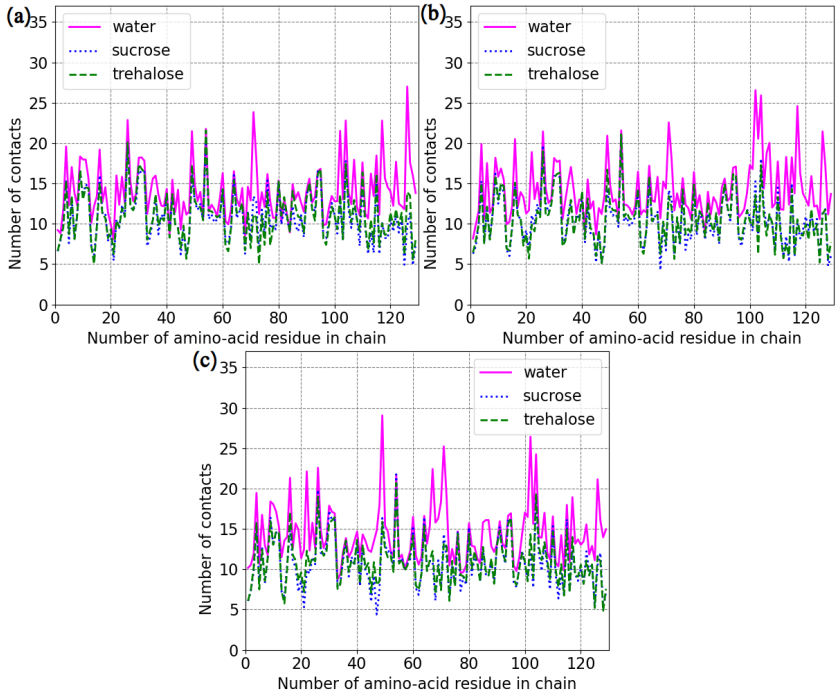

Figure 6: Average number of contacts per amino-acid residue per protein molecule. (a) Systems: LYS., LYS.+SUC., LYS.+TRE. (b) Systems: LYS.+NaCl, LYS.+SUC.+NaCl, LYS.+TRE.+NaCl. (c) Systems: LYS.+$ZnCl_2$, LYS.+SUC.+$ZnCl_2$, LYS.+TRE.+$ZnCl_2$. "Water" stands for systems without disaccharides.

Table 3: Average number of contacts per amino-acid residue.

System	Average number of contacts per amino-acid residue
LYS.	14.00 ± 3.45
LYS.+SUC.	10.87 ± 3.13
LYS.+TRE.	11.07 ± 3.14
LYS.+NaCl	14.22 ± 3.54
LYS.+SUC.+NaCl	10.46 ± 3.15
LYS.+TRE.+NaCl	10.54 ± 3.12
LYS.+$ZnCl_2$	14.39 ± 3.67
LYS.+SUC.+$ZnCl_2$	10.79 ± 3.22
LYS.+TRE.+$ZnCl_2$	11.01 ± 2.99

An additional information about the interactions between protein molecules and disaccharides can be obtained from RDFs (which is also g(r)) between centers of mass of disaccharides and amino-acid residues.

Figure 7 demonstrates such RDFs for every studied mixture with sucrose and trehalose. Despite similar appearances of patterns, there are differences. In mixtures without salts trehalose and sucrose associate with roughly 54 amino-acid residues. When NaCl is present the number of associated amino-acid residues with sucrose is 66 while for trehalose it is 57. In $ZnCl_2$ sucrose can possibly bind to 52 residues, while this number for trehalose is 47. Thus, overall sucrose binds slightly more amino-acid residues.

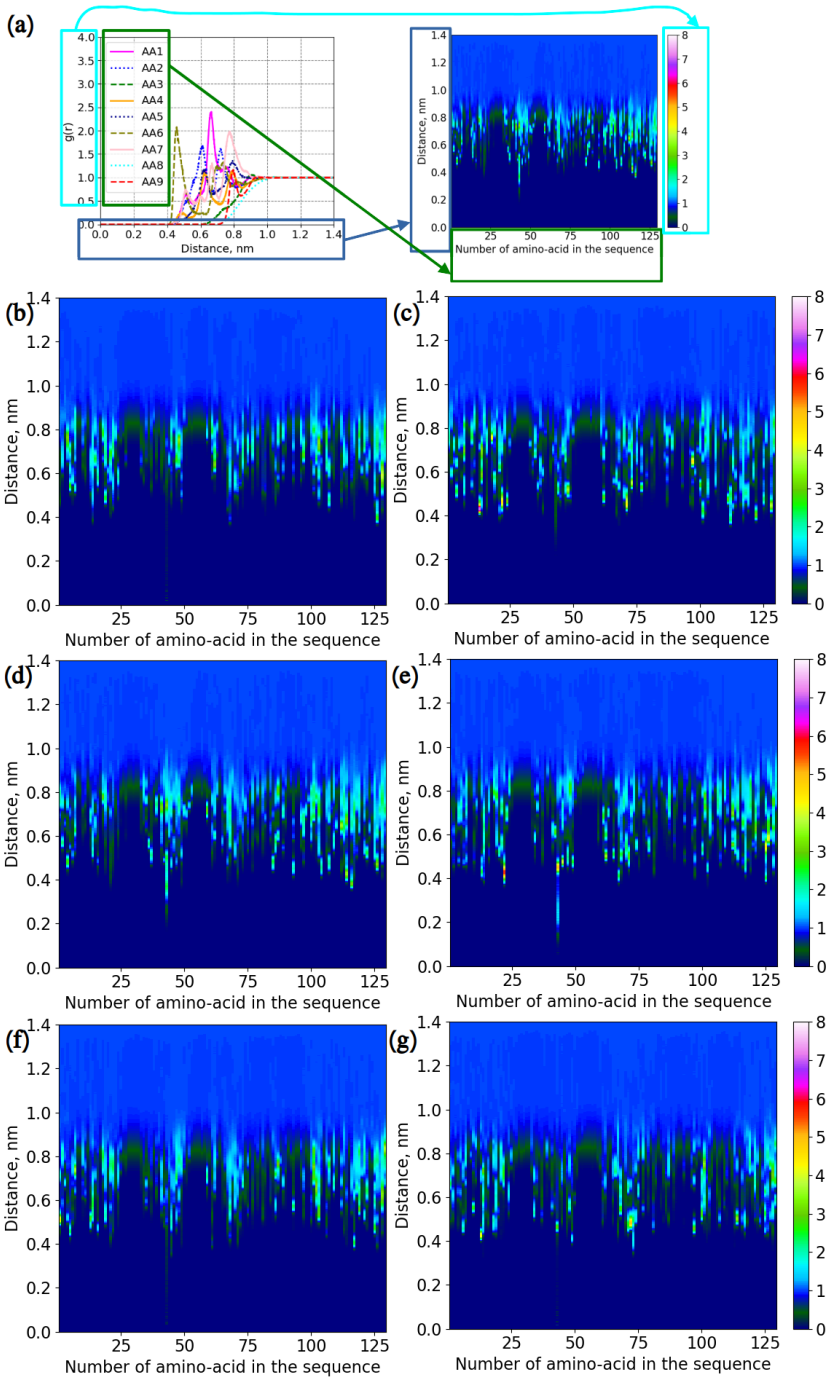

Figure 7: RDFs for protein-disaccharide interactions, computed between centers of mass of amino-acid residues and disaccharides. (a) Illustration of how colormaps were created. (b) System LYS.+SUC. (c) System LYS.+TRE. (d) System LYS.+SUC.+NaCl. (e) System LYS.+TRE.+NaCl. (f) System LYS.+SUC.+$ZnCl_2$. (g)System LYS.+TRE.+$ZnCl_2$.

Coarse-grained MD simulations

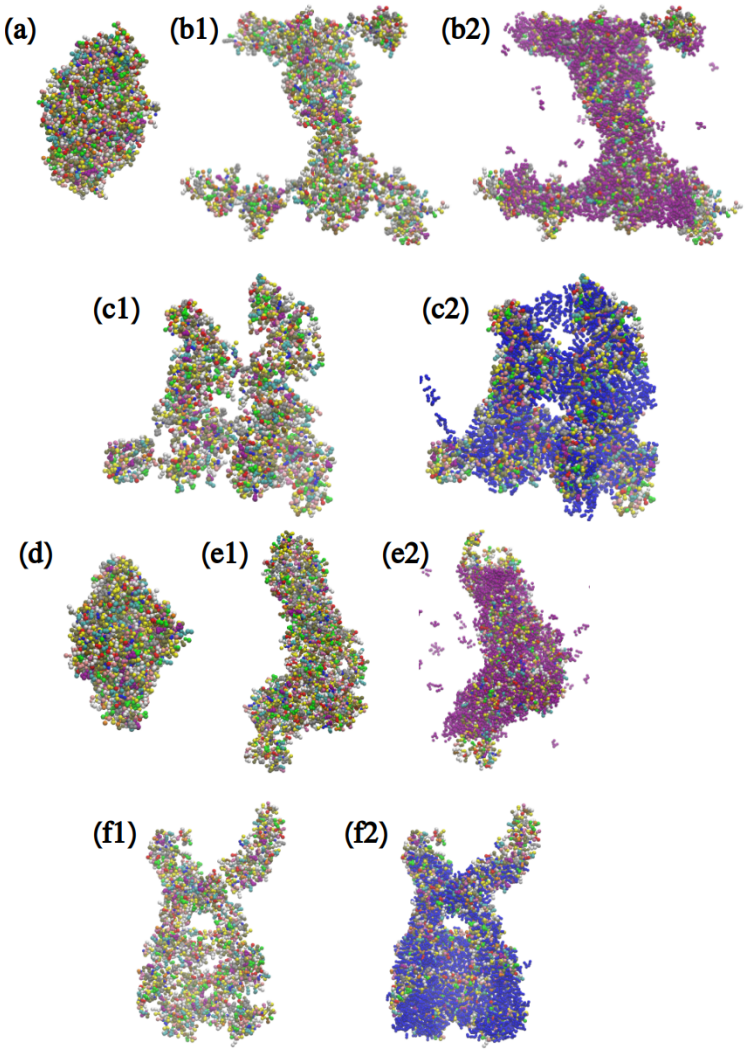

Figure 8: Snapshots from coarse-grained simulations. (a) Lys.+NaCl. (b1) Lys.+Suc.+NaCl (sucrose is omitted). (b2) Lys.+Suc.+NaCl. (c1) Lys.+Tre.+NaCl (trehalose is omitted). (c2)Lys.+Tre.+NaCl. (d) Lys.+$CaCl_2$. (e1) Lys.+Suc.+$CaCl_2$ (sucrose is omitted). (e2) Lys.+Suc.+$CaCl_2$. (f1) Lys.+Tre.+$CaCl_2$ (trehalose is omitted). (f2) Lys.+Tre.+$CaCl_2$. Water and ions are omitted in all snapshots for clarity. Sucrose is presented as purple balls and trehalose is presented as blue balls. Proteins are presented as mixtures of balls of different colors.

Snapshots of the simulated systems are presented in Figure 8. For mixtures with disaccharides two kinds of images were made: one without them and another one with their presence. The lysozyme molecules form aggregates in both aqueous solutions without disaccharides (Figure 8 (a) and (d)). The addition of the disaccharides changes the behavior of

lysozyme: instead of globular aggregates, structures of more complex topologies appeared during the simulations. In mixtures with sucrose, clusters (Figure 8 (b1), (b2) and (e1), (e2)) are elongated through the simulation box, while in systems with trehalose (Figure 8 (c1), (c2) and (f1), (f2)) the structures of those cluster are broad. The fact that larger and more complex structures can be observed instead of globular accumulates implies that disaccharides locate themselves between protein molecules, which results in different topologies depending on if there is sucrose or trehalose in the mixture.

RMSDs for proteins

Since a part of the trajectory was used for further equilibration, RMSDs were computed for the last 50 μs.

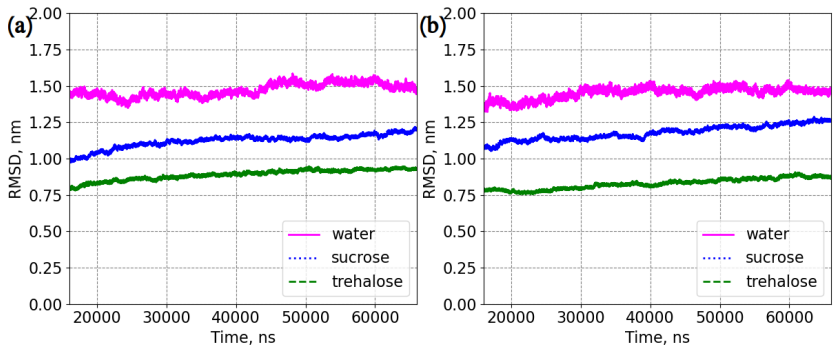

Figure 9: Averaged RMSDs for the coarse-grained systems. (a) Systems with NaCl. (b) Systems with $CaCl_2$. RMSDs for separate protein molecules can be observed in Figures S13-S14 of ESI.

Structures in coarse-grained simulations are different from atomistic ones: they have less amount of particles, there are no hydrogen bonds, since there are no hydrogen atoms, and there are no defined secondary structures. Therefore RMSDs have values of different order, compared to values obtained from atomistic simulations. Figure 9 shows average RMSDs for the simulated systems, using coarse-grained representations. Trehalose appears to be a supperior stabilizer as the average RMSD for the protein appears to be the lowest. The highest RMSD is obtained for lysozyme in aqueous solutions without any disaccharide.

Number of contacts and RDFs

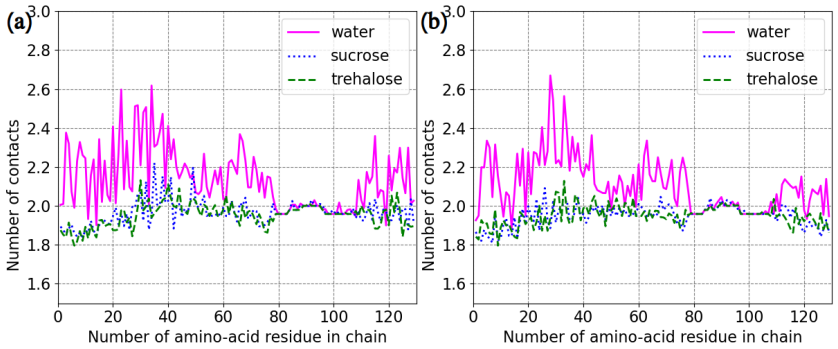

Figure 10: Number of contacts for each amino-acid residue per protein molecule for the coarse-grained systems. (a) Systems with NaCl. (b) Systems with $CaCl_2$.

As coarse-grained models contain smaller number of particles, the numbers of contacts is also smaller, compared to numbers from atomistic systems. Figure 10 demonstrates average number of contacts per amino-acid residue in the simulated mixtures. From the figure it follows that there are more contacts between protein molecules in aqueous solutions of lysozyme than in the systems with disaccharides. This is coherent with the conclusion made from the snapshots of the systems. Additionally, as with atomistic simulations, in coarse-grained systems the smallest variations of the number of contacts were observed for residues 80-100, comparing mixtures for both kinds of salts. However, also in this case the average number of contacts per grain and per amino-acid residue appears to be rather similar for all systems if the large standard deviations are taken into account (Table 4).

Table 4: Average number of contacts per amino-acid residue.

System	Average number of contacts per amino-acid residue
Lys.+NaCl	2.14 ± 0.72
Lys.+Suc.+NaCl	1.96 ± 0.24
Lys.+Tre.+NaCl	1.95 ± 0.21
Lys.+$CaCl_2$	2.11 ± 0.63
Lys.+Suc.+$CaCl_2$	1.95 ± 0.21
Lys.+Tre.+$CaCl_2$	1.95 ± 0.21

Considering the observations from RMSD and numbers of contacts, it is interesting to

find out if there are any preferential amino-acid residues which associate with molecules of disaccharides. The RDFs in Figure 11 demonstrate protein-disaccharide interactions. In contrary to the atomistic simulations, all residues associate similarly, i.e. the maximum values of g(r), which are also above 1, appear at the same distance of 0.5 nm. This can also be explained by smaller sizes of grains compared to similar molecular parts in the atomistic representation, which results in the lower spatial resolution.

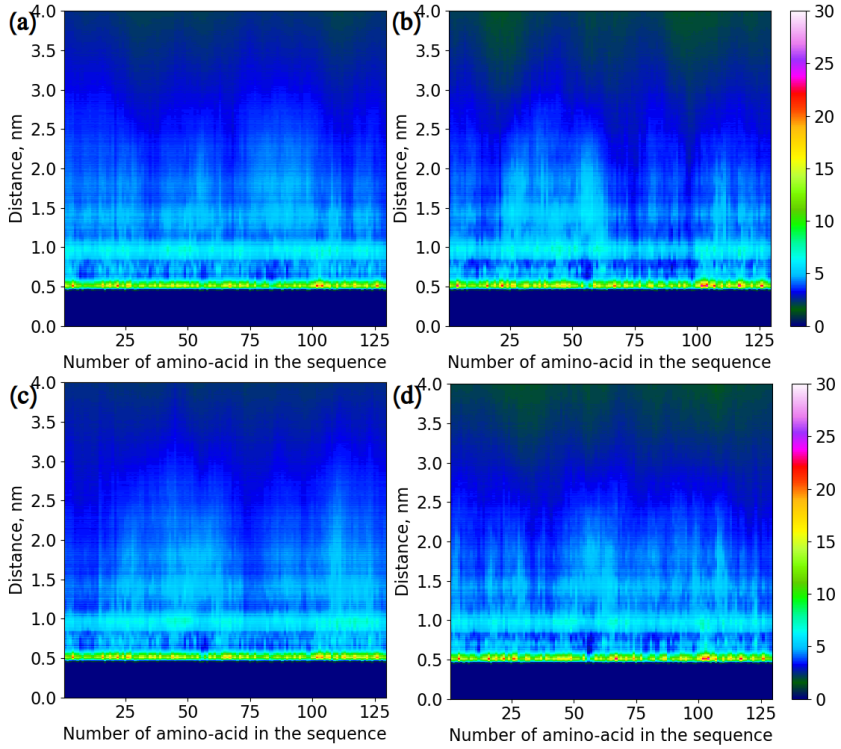

Figure 11: RDFs between centers of mass of disaccharides and amino-acid residues for the coarse-grained simulations. (a) Lys.+Suc.+NaCl. (b) Lys.+Tre.+NaCl. (c) Lys.+Suc.+$CaCl_2$. (d) Lys.+Tre.+$CaCl_2$. The colorbar on the right hand's side represents values of g(r).

Discussion

The presented data in atomistic simulations indicates that trehalose can be a better agent for slowing down the dynamics of systems with lysozyme. In order to understand why this happens and detect potential mechanisms, one needs to investigate possible correlations in the

presented data to correlate dynamic stability of the protein with structural characteristics.

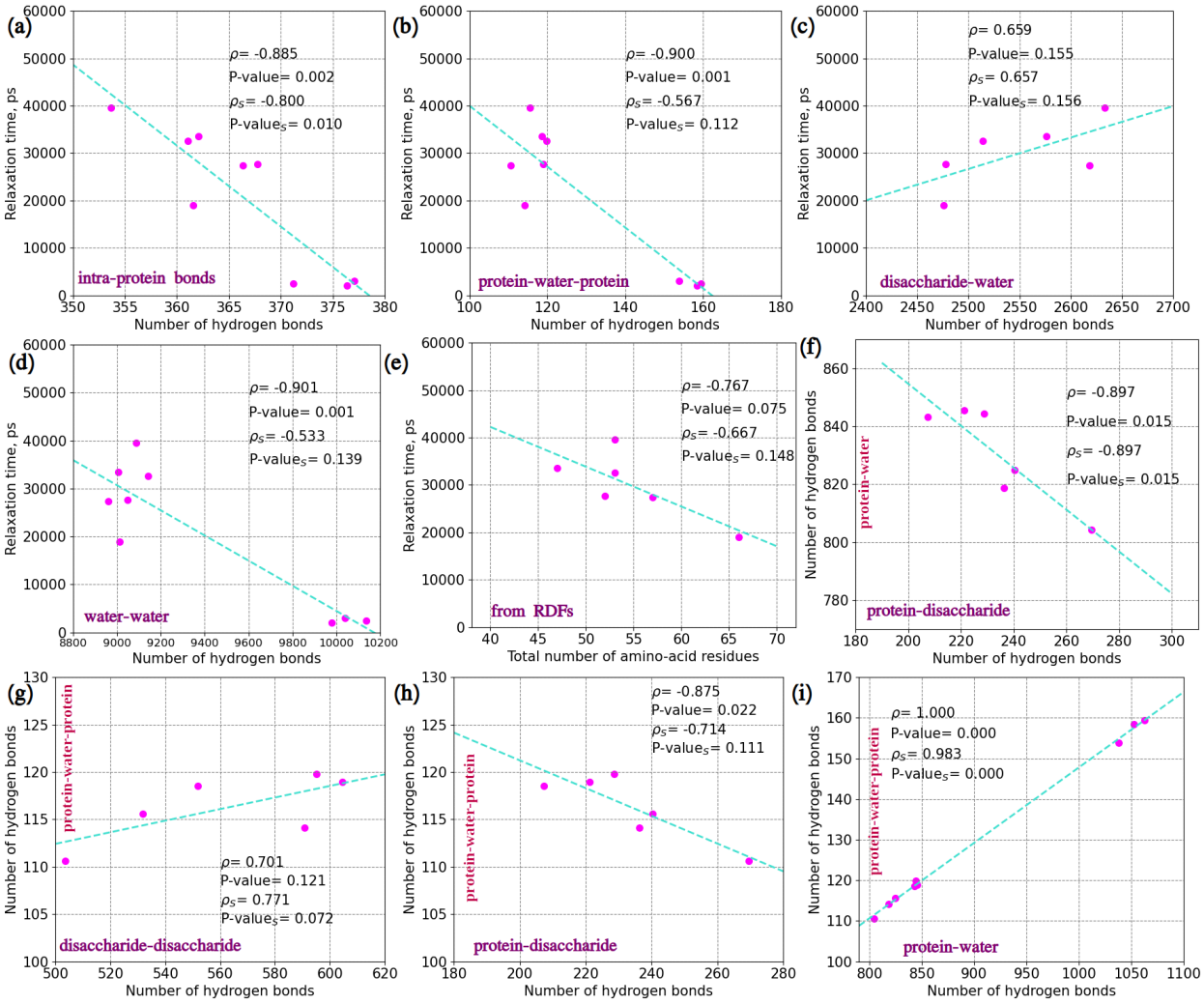

Figure 12: Correlations. (a) Relaxation times and number of intra-protein hydrogen bonds. (b) Relaxation times and number of protein-water-protein bridging hydrogen bonds. (c) Relaxation times and number of disaccharide-water hydrogen bonds. (d) Relaxation times and number of water-water hydrogen bonds. (e) Relaxation times and the total number of amino-acid residues associated (data from RDFs) with disaccharides. (f) Protein-disaccharide and protein-water hydrogen bonds. (g) Disaccharide-disaccharide and protein-water-protein bridging hydrogen bonds. (h) Protein-disaccharide and protein-water-protein bridging hydrogen bonds. (i) Protein-water and protein-water-protein bridging hydrogen bonds. Relaxation times were computed for q=15.71 nm^{-1}. Here ρ is the Pearson's correlation coefficient and P-value is the probability for the correlation being wrong. ρ_S is the Spearman's correlation coefficient and P-value$_S$ is the probability for the correlation being wrong. Pink points represent the data-points, turquoise lines are fitting lines.

For providing proper statistical determinations for this discussion well-known Pearson's

and Spearman's correlations were utilized. Figure 12 demonstrates significant correlations obtained from the presented data.

From Figures 12 (a) and (b) and high absolute values of Pearson's and Spearman's correlation coefficients together with their low P-values it follows, that the protein relaxation time is strongly dependent on internal bonds in the protein molecules, including the bridging bonds where water and ions can act as possible bridges[79,80] between atoms of lysozyme: the dynamics of the protein backbone is slower when there are less intra-molecular and internal bridging hydrogen bonds. Thus, the disaccharide molecules are not only disrupting the protein hydration shell, and slowing down its dynamics, but also reducing the number of internal hydrogen bonds in the protein. This is an important finding for understanding how disaccharides reduce protein dynamics and stabilize proteins.

Another important relation to the protein relaxation time is the strong positive correlation with disaccharide-water hydrogen bonds presented in Figure 12(c): a higher number of those bonds is related to a longer relaxation time. Consequently, this describes the potential ability to dehydrate the internal protein structure and contribute to the result shown in Figure 12(b). However, recalling conclusions from the work by R. D. Lins et al.[41] and considering the numbers of protein-water hydrogen bonds, it can also be deduced that the disaccharides act as a coating around the lysozyme, rather than as a dehydrating agent, which can also be a reason behind the slower relaxation of the internal protein structure.

It is known that the dynamics of water has an effect on other components of biological systems. There are more hydrogen bonds in more diluted systems, which leads to faster protein dynamics. Figure 12(d) exhibits the strong negative Pearson's and Spearman's correlations between the number of water-water hydrogen bonds and the relaxation time, which is fully consistent with the literature.

The last strong negative correlation with the relaxation time is with the number of associated amino-acid residues, obtained from RDFs: the disaccharide with the highest ability to inhibit the dynamics of lysozyme's backbone is the one which binds to less residues,

which is trehalose (Figure 12(e)).

In order to disclose more details on mechanisms of protein stabilisation, correlations between hydrogen bonds were calculated as well. Figure 12(f) shows a strong negative correlation between protein-disaccharide and protein-water hydrogen bonds: there are less protein-water hydrogen bonds in systems with more protein-disaccharide hydrogen bonds, which is a natural consequence of that disaccharide molecules replace water molecules at the protein surface.

Protein-water-protein bridging (or bifurcated) hydrogen bonds are in strong positive and strong negative correlations with disaccharide-disaccharide and protein-disaccharide hydrogen bonds respectively (Figures 12(g) and (h)). This is also a consequence of that hydroxyl groups of the disaccharides are replacing water molecules in the protein hydration shell, without becoming bridging units themselves, which thereby decreases the number of those bifurcated hydrogen bonds. This is also confirmed by a strong positive correlation between the bridging hydrogen bonds and the protein-water hydrogen bonds (Figure 12(i)).

Finalizing this discussion regarding the atomistic simulations, mechanisms of lysozyme preservation can be proposed for the studied mass ratios of protein, disaccharides, water and ions. In the simulated systems a well-preserved lysozyme is the one with the smallest number of intra-molecular hydrogen bonds. Thus, the stabilised backbone is less hydrated, compared to less stable structures, where more bridging (bifurcated) hydrogen bonds with water can be observed. This implies that hydroxyl groups of the disaccharides replace and bind water from the hydration shell of the protein, which results in a suppressed dynamics of the shell, as disaccharides are known to have slower movements than water,[81] followed by inhibited motions of the protein.[82] Therefore, sucrose/trehalose together with water molecules form protective layers around the protein molecules, which is insuring the protein preservation.

Trehalose has properties which are better to stabilise lysozyme structure than sucrose at the studied protein-sugar mass ratios. On the other hand, if there is a strong demand to use sucrose as a preservative for lysozyme, then it is valuable to consider its combination with

zinc ions which have an ability to improve the performance of sucrose.

From coarse-grained simulations trehalose appeared to be the superior stabilizer as well. Despite that no exact mechanisms can be disclosed due to low resolution of coarse-grained models, out of presented results and snapshots it can be concluded that trehalose has a somewhat larger ability to prevent aggregation of the protein than sucrose.

Conclusions

MD simulations on atomistic and coarse-grained levels were performed in this work for aqueous solutions of lysozyme with disaccharides and/or various salts. The results show that trehalose slows down the protein dynamics more than sucrose and the reason for this seems to be that trehalose forms more hydrogen bonds to water and thereby disrupts the protein hydration water more than sucrose. Sucrose binds to more amino-acid residues than trehalose, but it can not form hydrogen bonds to the same amount of water as trehalose due to that sucrose has a stronger affinity to itself, as shown earlier by I. Ermilova et al.[78] The stronger hydrogen bonding of trehalose to water, seems, in turn, to result in a reduced number of internal protein hydrogen bonds, both with and without bridging water molecules. Thus, somewhat surprisingly, there is a strong correlation between an increasing protein relaxation time and a decreasing number of internal protein hydrogen bonds. This is an important finding for understanding the rules of disaccharides in general and trehalose in particular for protein stabilization. The addition of the disaccharides to the protein solution seems to have a similar effect on the protein dynamics as a dehydration of the protein, without causing the detrimental effects of dehydration.

Effects of the presence of salts or counter ions on protein dynamics were also disclosed. The slowest relaxation of lysozyme is observed when salts are absent and only counter ions of Cl^- are added to the mixtures, while the fastest motion of the protein is seen in the presence of NaCl. Moreover, ions affect the ability of disaccharides to separate different protein

molecules and thereby prevent protein aggregation. In mixtures with only Cl^- counter ions and with $ZnCl_2$, sucrose prevents aggregation of lysozyme better than trehalose. In fact, Zn^{2+} ions are known as inhibitors of amyloid fibril formation of hen egg-white lysozyme.[83] A combination of these ions and lysozyme have also shown antimicrobial activities.[74] Therefore, it is valuable to consider lysozyme, encapsulated with the help of sucrose and Zn^{2+} ions, for pharmaceutical applications.

In the case of protein solutions with trehalose, protein aggregation is most effectively prevented by adding NaCl. This is also an important finding since NaCl is the most common salt in physiological systems and furthermore used by the computational community to mimic the physiological acidity of the environment.

To summarize, the findings we have obtained in this study are important for understanding how proteins in e.g. pharmaceuticals should be stabilized for maintaining the desired properties over time.

Conflicts of interest

There are no conflicts to declare.

Acknowledgement

We would like to thank Linnea Ögren for running MD simulations.

The computations were performed on resources provided by the Swedish National Infrastructure for Computing (SNIC). In High Performance Computing Center North (HPC2N) Kebnekaise cluster was used for simulations with the project numbers SNIC2019/5-74 and SNIC2020/5-45 and the storage was given in terms of projects SNIC2020/10-22 and SNIC2020/6-53. We are grateful to National Academic Infrastructure for Supercomputing in Sweden (NAISS) for computational time from projects NAISS 2024/5-434, NAISS 2024/22-667, NAISS 2024/22-666, which was used for additional analysis. Finally, this work was financially

supported by the Swedish Research Council (Vetenskapsrådet), grant no. 2019-04020.

Author Information

Corresponding Author

Inna Ermilova: inna.ermilova@chalmers.se ; ina.ermilova@gmail.com.

Notes

The authors declare no competing financial interest.

References

(1) Nasilowska-Adamska, B.; Rzepecki, P.; Manko, J.; Czyz, A.; Markiewicz, M.; Fedorowicz, I.; Tomaszewska, A.; Piatkowska-Jakubas, B.; Wrzesien-Kus, A.; Bieniaszewska, M.; others The Significance of Palifermin (Kepivance) in Reduction of Oral Mucositis (OM) Incidence and Acute Graft Versus Host Disease (aGvHD) in Patients with Hematological Diseases Undergoing HSCT. *Blood* **2006**, *108*, 2965.

(2) Wang, W.; Ohtake, S. Science and art of protein formulation development. *Int. J. Pharm.* **2019**, *568*, 118505.

(3) J.Singh; M.Peric Interation of the β-amyloid - A$\beta(25-35)$ - peptide with zwitterionic and negatively charged vesicles with and without cholesterol. *Chem. Phys. Lipids* **2018**, *216*, 39 – 47.

(4) Patist, A.; Zoerb, H. Preservation mechanisms of trehalose in food and biosystems. *Colloids Surf. B Biointerfaces* **2005**, *40*, 107–113.

(5) Kon, E.; Elia, U.; Peer, D. Principles for designing an optimal mRNA lipid nanoparticle vaccine. *Curr. Opin. Biotechnol.* **2022**, *73*, 329–336.

(6) Marycz, K.; Grzesiak, J.; Hill-Bator, A.; Misiuk-Hojo, M. Protection Capability Of Hyaluronan-containing Artificial Tear Drops Against Desiccation On Cultured Human Corneal Epithelial Cells. *Invest. Ophthalmol. Vis. Sci.* **2012**, *53*, 582–582.

(7) Aboagla, E. M.-E.; Terada, T. Trehalose-enhanced fluidity of the goat sperm membrane and its protection during freezing. *Biol. Reprod.* **2003**, *69*, 1245–1250.

(8) Hincha, D. K. Low concentrations of trehalose protect isolated thylakoids against mechanical freeze-thaw damage. *Biochim. Biophys. Acta-Biomembranes* **1989**, *987*, 231–234.

(9) Zhang, M.; Oldenhof, H.; Sydykov, B.; Bigalk, J.; Sieme, H.; Wolkers, W. F. Freeze-drying of mammalian cells using trehalose: preservation of DNA integrity. *Sci. Rep.* **2017**, *7*, 6198.

(10) Rockinger, U.; Funk, M.; Winter, G. Current approaches of preservation of cells during (freeze-) drying. *J. Pharm. Sci.* **2021**, *110*, 2873–2893.

(11) Ohtake, S.; Wang, Y. J. Trehalose: current use and future applications. *J. Pharm. Sci.* **2011**, *100*, 2020–2053.

(12) Newman, Y.; Ring, S.; Colaco, C. The role of trehalose and other carbohydrates in biopreservation. *Biotechnol. Genet. Eng. Rev.* **1993**, *11*, 263–294.

(13) Jones, K. L.; Drane, D.; Gowans, E. J. Long-term storage of DNA-free RNA for use in vaccine studies. *Biotechniques* **2007**, *43*, 675–681.

(14) Bakaltcheva, I.; O'Sullivan, A. M.; Hmel, P.; Ogbu, H. Freeze-dried whole plasma: evaluating sucrose, trehalose, sorbitol, mannitol and glycine as stabilizers. *Thromb. Res.* **2007**, *120*, 105–116.

(15) Ball, R. L.; Bajaj, P.; Whitehead, K. A. Achieving long-term stability of lipid nanoparticles: examining the effect of pH, temperature, and lyophilization. *IInt. J. Nanomedicine* **2017**, 305–315.

(16) Luo, W.-C.; Beringhs, A. O.; Kim, R.; Zhang, W.; Patel, S. M.; Bogner, R. H.; Lu, X. Impact of formulation on the quality and stability of freeze-dried nanoparticles. *Eur. J. Pharm. Biopharm.* **2021**, *169*, 256–267.

(17) Wang, T.; Sung, T.-C.; Yu, T.; Lin, H.-Y.; Chen, Y.-H.; Zhu, Z.-W.; Gong, J.; Pan, J.; Higuchi, A. Next-generation materials for RNA–lipid nanoparticles: lyophilization and targeted transfection. *J. Mater. Chem. B* **2023**, *11*, 5083–5093.

(18) Noji, M.; Samejima, T.; Yamaguchi, K.; So, M.; Yuzu, K.; Chatani, E.; Akazawa-Ogawa, Y.; Hagihara, Y.; Kawata, Y.; Ikenaka, K.; others Breakdown of supersaturation barrier links protein folding to amyloid formation. *Commun. Biol.* **2021**, *4*, 120.

(19) Deckers, D.; Vanlint, D.; Callewaert, L.; Aertsen, A.; Michiels, C. W. Role of the Lysozyme Inhibitor Ivy in Growth or Survival of Escherichia coli and Pseudomonas aeruginosa Bacteria in Hen Egg White and in Human Saliva and Breast Milk. *Applied and Environmental Microbiology* **May. 2008**, *74*, 4434–4439.

(20) Ganz, T. *Encyclopedia of Respiratory Medicine*; Academic Press, 2006; pp 649–653.

(21) Cao, D.; Wu, H.; Li, Q.; Sun, Y.; Liu, T.; Fei, J.; Zhao, Y.; Wu, S.; Hu, X.; Li, N. Expression of recombinant human lysozyme in egg whites of transgenic hens. *PloS one* **2015**, *10*, e0118626.

(22) Ferraboschi, P.; Ciceri, S.; Grisenti, P. Applications of Lysozyme, an Innate Immune Defense Factor, as an Alternative Antibiotic. *Antibiotics 10*.

(23) Vettore, N.; Moray, J.; Brans, A.; Herman, R.; Charlier, P.; Kumita, J. R.; Kerff, F.; Dobson, C. M.; Dumoulin, M. Characterisation of the structural, dynamic and aggrega-

tion properties of the W64R amyloidogenic variant of human lysozyme. *Biophys. Chem.* **2021**, *271*, 106563.

(24) Sziegat, F.; Wirmer-Bartoschek, J.; Schwalbe, H. Characteristics of Human Lysozyme and Its Disease-Related Mutants in their Unfolded States. *Angew. Chem.* **2011**, *50*, 5514–5518.

(25) Kumari, P.; Kumari, M.; Kashyap, H. K. How Pure and Hydrated Reline Deep Eutectic Solvents Affect the Conformation and Stability of Lysozyme: Insights from Atomistic Molecular Dynamics Simulations. *J. Phys. Chem. B 124*.

(26) Gibrat, J.-F.; Gō, N. Normal mode analysis of human lysozyme: Study of the relative motion of the two domains and characterization of the harmonic motion. *Proteins: Struct., Funct., Bioinf.* **1990**, *8*, 258–279.

(27) Oda, M.; Sano, T.; Kamatari, Y. O.; Abe, Y.; Ikura, T.; Ito, N. Structural Analysis of Hen Egg Lysozyme Refolded after Denaturation at Acidic pH. *Protein. J.* **2022**, *41*, 71–78.

(28) Phan-Xuan, T.; Bogdanova, E.; Sommertune, J.; Fureby, A. M.; Fransson, J.; Terry, A. E.; Kocherbitov, V. The role of water in the reversibility of thermal denaturation of lysozyme in solid and liquid states. *Biochem. Biophys. Rep.* **2021**, *28*, 101184.

(29) Jiang, L.; Li, Y.; Wang, L.; Guo, J.; Liu, W.; Meng, G.; Zhang, L.; Li, M.; Cong, L.; Sun, M. Recent insights into the prognostic and therapeutic applications of lysozymes. *Front. Pharmacol* **2021**, *12*, 767642.

(30) Bergamo, A.; Sava, G. Lysozyme: A Natural Product with Multiple and Useful Antiviral Properties. *Molecules* **2024**, *29*, 652.

(31) Maidment, C.; Dyson, A.; Beard, J. A study into measuring the antibacterial activity of lysozyme-containing foods. *Nutr. Food Sci.* **2009**, *39*, 29–35.

(32) Zimoch-Korzycka, A.; Gardrat, C.; Castellan, A.; Coma, V.; Jarmoluk, A. The use of lysozyme to prepare biologically active chitooligomers. *Polímeros* **2015**, *25*, 35–41.

(33) Shahmohammadi, A. Lysozyme separation from chicken egg white: a review. *Eur. Food Res. Technol.* **2018**, *244*, 577–593.

(34) Phan-Xuan, T.; Bogdanova, E.; Millqvist Fureby, A.; Fransson, J.; Terry, A. E.; Kocherbitov, V. Hydration-induced structural changes in the solid state of protein: A SAXS/WAXS study on lysozyme. *Mol. Pharmaceutics* **2020**, *17*, 3246–3258.

(35) Ahlgren, K.; Havemeister, F.; Andersson, J.; Esbjörner, E. K.; Swenson, J. The inhibition of fibril formation of lysozyme by sucrose and trehalose. *RSC Adv.* **2024**, *14*, 11921–11931.

(36) Jonsson, O.; Lundell, A.; Rosell, J.; You, S.; Ahlgren, K.; Swenson, J. Comparison of Sucrose and Trehalose for Protein Stabilization Using Differential Scanning Calorimetry. *J. Phys. Chem. B* **2024**,

(37) Bogdanova, E.; Lages, S.; Phan-Xuan, T.; Kamal, M. A.; Terry, A.; Millqvist Fureby, A.; Kocherbitov, V. Lysozyme–Sucrose Interactions in the Solid State: Glass Transition, Denaturation, and the Effect of Residual Water. *Mol. Pharmaceutics.* **2023**, *20*, 4664–4675.

(38) Magazù, S.; Migliardo, F.; Benedetto, A.; Mondelli, C.; Gonzalez, M. A. Thermal behaviour of hydrated lysozyme in the presence of sucrose and trehalose by EINS. *J. Non-Cryst. Solids* **2011**, *357*, 664–670.

(39) Starciuc, T.; Malfait, B.; Danede, F.; Paccou, L.; Guinet, Y.; Correia, N. T.; Hedoux, A. Trehalose or sucrose: which of the two should be used for stabilizing proteins in the

solid state? A dilemma investigated by in situ micro-raman and dielectric relaxation spectroscopies during and after freeze-drying. *J. Pharm. Sci.* **2020**, *109*, 496–504.

(40) Lerbret, A.; Affouard, F.; Bordat, P.; Hédoux, A.; Guinet, Y.; Descamps, M. Molecular dynamics simulations of lysozyme in water/sugar solutions. *Chem. Phys.* **2008**, *345*, 267–274.

(41) Lins, R. D.; Pereira, C. S.; Hünenberger, P. H. Trehalose–protein interaction in aqueous solution. *Proteins: Struct., Funct., Bioinf.* **2004**, *55*, 177–186.

(42) Fedorov, M. V.; Goodman, J. M.; Nerukh, D.; Schumm, S. Self-assembly of trehalose molecules on a lysozyme surface: the broken glass hypothesis. *Phys. Chem. Chem. Phys.* **2011**, *13*, 2294–2299.

(43) Simončič, M.; Lukšič, M. Mechanistic differences in the effects of sucrose and sucralose on the phase stability of lysozyme solutions. *J. Mol. Liq.* **2021**, *326*, 115245.

(44) Huang, J.; Jr, A. D. M. CHARMM36 All-Atom Additive Protein Force Field: Validation Based on Comparison to NMR Data. *J. Comput. Chem.* **2013**, *34*, 2135–2145.

(45) Ahlgren, K.; Olsson, C.; Ermilova, I.; Swenson, J. New insights into the protein stabilizing effects of trehalose by comparing with sucrose. *Phys. Chem. Chem. Phys.* **2023**, *25*, 21215–21226.

(46) Jorgensen, W. L.; Jenson, C. Temperature dependence of TIP3P, SPC, and TIP4P water from NPT Monte Carlo simulations: Seeking temperatures of maximum density. *J. Comput. Chem.* **1998**, *19*, 1179–1186.

(47) Jorgensen, W. L.; Chandrasekhar, J.; Madura, J. D.; Impey, R. W.; Klein, M. L. Comparison of simple potential functions for simulating liquid water. *J. Chem. Phys.* **1983**, *79*, 926–935.

(48) Spoel, D. V. D.; Lindahl, E.; Hess, B.; Groenhof, G.; Mark, A. E.; Berendsen, H. J. C. GROMACS: fast, flexible, and free. *J. Comput. Chem.* **2005**, *26*, 1701–1718.

(49) Salsburg, Z. W. Statistical-Mechanical Properties of Small Systems in the Isothermal—Isobaric Ensemble. *J. Chem. Phys.* **1966**, *44*, 3090–3094.

(50) Van Gunsteren, W. F.; Berendsen, H. J. A leap-frog algorithm for stochastic dynamics. *Mol. Sim.* **1988**, *1*, 173–185.

(51) Berendsen, H. J. C.; Postma, J. P. M.; van Gunsteren, W. F.; Nola, A. D.; Haak, J. R. Molecular dynamics with coupling to an external bath. *J. Chem. Phys.* **1984**, *81*, 3684 – 3690.

(52) Bussi, G.; Donadio, D.; Parrinello, M. Canonical sampling through velocity rescaling. *J. Chem. Phys.* **2007**, *126*, 014101.

(53) Grubmüller, H.; Heller, H.; Windemuth, A.; Schulten, K. Generalized Verlet algorithm for efficient molecular dynamics simulations with long-range interactions. *Mol. Simul.* **1991**, *6*, 121–142.

(54) Hess, B.; Bekker, H.; Berendsen, H. J.; Fraaije, J. G. LINCS: a linear constraint solver for molecular simulations. *J. Comput. Chem.* **1997**, *18*, 1463–1472.

(55) Darden, T.; York, D.; Pedersen, L. Particle mesh Ewald: An N log (N) method for Ewald sums in large systems. *J. Chem. Phys.* **1993**, *98*, 10089–10092.

(56) Gibbs, J. W. *Elementary principles in statistical mechanics: developed with especial reference to the rational foundations of thermodynamics*; C. Scribner's sons, 1902.

(57) Jo, S.; Cheng, X.; Lee, J.; Kim, S.; Park, S.-J.; Patel, D. S.; Beaven, A. H.; Lee, K. I.; Rui, H.; Park, S.; others CHARMM-GUI 10 years for biomolecular modeling and simulation. *J. Comput. Chem.* **2017**, *38*, 1114–1124.

(58) Souza, P. C.; Alessandri, R.; Barnoud, J.; Thallmair, S.; Faustino, I.; Grünewald, F.; Patmanidis, I.; Abdizadeh, H.; Bruininks, B. M.; Wassenaar, T. A.; others Martini 3: a general purpose force field for coarse-grained molecular dynamics. *Nat. Methods* **2021**, *18*, 382–388.

(59) Onsager, L. Electric moments of molecules in liquids. *J. Am. Chem. Soc.* **1936**, *58*, 1486–1493.

(60) van Gunsteren, W. F.; Berendsen, H. J.; Rullmann, J. A. Inclusion of reaction fields in molecular dynamics. Application to liquid water. *Faraday Discuss. Chem. Soc.* **1978**, *66*, 58–70.

(61) Gil-Villegas, A.; McGrother, S. C.; Jackson, G. Reaction-field and Ewald summation methods in Monte Carlo simulations of dipolar liquid crystals. *Mol. Phys.* **1997**, *92*, 723–734.

(62) Parrinello, M.; Rahman, A. Crystal structure and pair potentials: A molecular-dynamics study. *Phys. Rev. Lett.* **1980**, *45*, 1196.

(63) Parrinello, M.; Rahman, A. Polymorphic transitions in single crystals: A new molecular dynamics method. *J. Appl. Phys.* **1981**, *52*, 7182–7190.

(64) Parrinello, M.; Rahman, A. Strain fluctuations and elastic constants. *J. Chem. Phys.* **1982**, *76*, 2662–2666.

(65) Bressert, E. SciPy and NumPy: an overview for developers. **2012**,

(66) Pajankar, A. *Python 3 Image Processing: Learn Image Processing with Python 3, NumPy, Matplotlib, and Scikit-image*; BPB Publications, 2019.

(67) Kowalski, C. J. On the effects of non-normality on the distribution of the sample product-moment correlation coefficient. *J. R. Stat. Soc., C: Appl. Stat* **1972**, *21*, 1–12.

(68) Akoglu, H. User's guide to correlation coefficients. *Turk. J. Emerg. Med.* **2018**, *18*, 91–93.

(69) Kendall, M. G. The advanced theory of statistics. **1943**,

(70) Van Hove, L. Correlations in space and time and Born approximation scattering in systems of interacting particles. *Phys. Rev.* **1954**, *95*, 249.

(71) Hansen, J.-P.; McDonald, I. R. *Theory of simple liquids: with applications to soft matter*; Academic press, 2013.

(72) Vineyard, G. H. Scattering of slow neutrons by a liquid. *Phys. Rev.* **1958**, *110*, 999.

(73) Gilbert, J.; Ermilova, I.; Nagao, M.; Swenson, J.; Nylander, T. Effect of encapsulated protein on the dynamics of lipid sponge phase: A neutron spin echo and molecular dynamics simulation study. *Nanoscale* **2022**, *14*, 6990–7002.

(74) Rogowska, A.; Król-Górniak, A.; Railean, V.; Kanawati, B.; Schmitt-Kopplin, P.; Michalke, B.; Sugajski, M.; Pomastowski, P.; Buszewski, B. Deciphering the complexes of zinc ions and hen egg white lysozyme: Instrumental analysis, molecular docking, and antimicrobial assessment. *Spectrochim. Acta A Mol. Biomol. Spectrosc.* **2024**, *305*, 123490.

(75) Rozas, I.; Alkorta, I.; Elguero, J. Bifurcated hydrogen bonds: three-centered interactions. *J. Phys. Chem. A* **1998**, *102*, 9925–9932.

(76) Feldblum, E. S.; Arkin, I. T. Strength of a bifurcated H bond. *Proc. Natl. Acad. Sci.* **2014**, *111*, 4085–4090.

(77) Motai, K.; Koishihara, N.; Narimatsu, T.; Ohtsu, H.; Kawano, M.; Wada, Y.; Akisawa, K.; Okuwaki, K.; Mori, T.; Kim, J.-S.; others Bifurcated Hydrogen Bonds in a Peptide Crystal Unveiled by X-ray Diffraction and Polarized Raman Spectroscopy. *Cryst. Growth Des.* **2023**, *23*, 4556–4561.

(78) Ermilova, I.; Lyubartsev, A.; Kocherbitov, V. Sucrose versus Trehalose: Observations from Comparative Study Using Molecular Dynamics Simulations. *ACS Omega* **2024**,

(79) Sindelar, C. V.; Hendsch, Z. S.; Tidor, B. Effects of salt bridges on protein structure and design. *Protein Sci.* **1998**, *7*, 1898–1914.

(80) Matsarskaia, O.; Roosen-Runge, F.; Schreiber, F. Multivalent ions and biomolecules: Attempting a comprehensive perspective. *ChemPhysChem* **2020**, *21*, 1742–1767.

(81) Magazù, S.; Migliardo, F.; Telling, M. Study of the dynamical properties of water in disaccharide solutions. *Eur. Biophys. J.* **2007**, *36*, 163–171.

(82) Frauenfelder, H.; Chen, G.; Berendzen, J.; Fenimore, P. W.; Jansson, H.; McMahon, B. H.; Stroe, I. R.; Swenson, J.; Young, R. D. A unified model of protein dynamics. *Proc. Natl. Acad. Sci.* **2009**, *106*, 5129–5134.

(83) Ma, B.; Zhang, F.; Wang, X.; Zhu, X. Investigating the inhibitory effects of zinc ions on amyloid fibril formation of hen egg-white lysozyme. *Int. J. Biol. Macromol.* **2017**, *98*, 717–722.